第 36 卷第 6 期 无 机 化 学 学 报 Vol.36 No.6
2020 年 6 月 CHINESE JOURNAL OF INORGANIC CHEMISTRY 1195-1203

一种氮烷基化的 2-(5-溴-4-甲基噻吩)-咪唑[4,5-*f*]-[1,10]-菲咯啉三羰基铼(I)配合物的聚集诱导荧光增强效应

彭雨新[1,2] 刘华奇[2,3] 胡 斌[3] 钱惠芬*[,1] 黄 伟*[,2,4]
([1]南京工业大学化学与分子工程学院,南京 210009)
([2]南京大学化学化工学院,配位化学国家重点实验室,南京 210023)
([3]南昌航空大学,江西省持续性污染物控制与资源循环利用重点实验室,南昌 330063)
([4]南京大学深圳研究院,深圳 518057)

摘要:本文旨在探索基于 2-噻吩-咪唑[4,5-*f*]-[1,10]-菲咯啉(TIP)结构的三羰基铼(I)配合物的聚集诱导荧光增强(AIEE)性质。研究了 2-(5-溴-4-甲基噻吩)-咪唑[4,5-*f*]-[1,10]-菲咯啉(**1**)与不同溴代烷烃之间的氮烷基化反应,并成功制备了 3 种具有不同氮烷基链结构的 TIP 衍生物(**2a~2c**)。氮烷基链引入可以明显提高其在有机溶剂中的溶解性以及不同程度影响 TIP 中相邻咪唑环和噻吩环的二面角。通过配体 **2a** 与五羰基氯化铼的配位反应成功制备了一个具有 AIEE 性质的三羰基铼(I)配合物 **3**。通过对三羰基铼(I)配合物 **3** 进行 X 射线单晶衍射的分析,发现该配合物的 AIEE 活性取决于其松弛的分子堆积结构以及多重的分子间氢键作用。

关键词:聚集诱导荧光增强;氮烷基化反应;三羰基铼配合物;单晶结构
中图分类号:O614.71+3 **文献标识码**:A **文章编号**:1001-4861(2020)06-1195-09
DOI:10.11862/CJIC.2020.130

An *N*-Alkylated 2-(5-Bromo-4-methylthiophen-2-yl)-imidazo[4,5-*f*]-[1,10]-phenanthroline Rhenium(I) Tricarbonyl Compound Showing Aggregation-Induced Emission Enhancement

PENG Yu-Xin[1,2] LIU Hua-Qi[2,3] HU Bin[3] QIAN Hui-Fen*[,1] HUANG Wei*[,2,4]
([1]*College of Chemistry and Molecular Engineering, Nanjing Tech University, Nanjing* 210009, *China*)
([2]*State Key Laboratory of Coordination Chemistry, School of Chemistry and Chemical Engineering, Nanjing University, Nanjing* 210093, *China*)
([3]*Key Laboratory of Jiangxi Province for Persistent Pollutants Control and Resources Recycle, Nanchang Hangkong University, Nanchang* 330063, *China*)
([4]*Shenzhen Research Institute of Nanjing University, Shenzhen, Guangdong* 518057, *China*)

Abstract: This work probes the aggregation-induced emission enhancement (AIEE) property of a 2-(2-thienyl) imidazo[4,5-*f*]-[1,10]-phenanthroline (TIP) based rhenium(I) tricarbonyl compound. Herein, *N*-alkylation reactions between 2-(5-bromo-4-methylthiophen-2-yl)-imidazo[4,5-*f*]-[1,10]-phenanthroline (**1**) and different alkyl bromides were carried out and three N-alkylated TIP derivatives (**2a~2c**) have been prepared successfully. The implantation of an *N*-alkyl group into the imidazole ring of TIP core can obviously increase the solubility in common organic solutions and affect the dihedral angles between imidazo [4,5-*f*][1,10]phenanthroline and its neighbouring thiophene ring to different extents. The AIEE active rhenium(I) tricarbonyl **3** was prepared via the reaction between **2a** and $Re(CO)_5Cl$. X-ray single-crystal analysis of **3** indicates that the loose packing mode and the multiple intermolecular

收稿日期:2020-03-23。收修改稿日期:2020-04-05。
国家自然科学基金(No.21871133),江苏省自然科学基金(No.BK20171334)和深圳市科技创新委员会项目(No.JCYJ20180307153251975)资助。
*通信联系人。E-mail:qhf@njtech.edu.cn,whuang@nju.edu.cn

hydrogen-bonding interactions are suggested to be responsible for the AIEE activity. CCDC: 1992191, **1**; 1992192, **2a**; 1992193, **2b**; 1992194, **2c**; 1992195, **3**.

Keywords: aggregation-induced emission enhancement; N-alkylation reaction; rhenium(I) tricarbonyl compound; single-crystal structure

The aggregation-induced emission (AIE) phenomenon has attracted various attentions in recent years due to its great significances in exploring the functional luminescence materials[1-3]. Generally, compounds with AIE nature could emit strong or moderate solid-state fluorescence, which is beneficial for the possible optoelectronic applications[4-6]. To date, many organic systems such as tetraphenylethene (TPE)[7], hexaphenylsilole (HPS)[8], cyano-stilbene[9], difluoroboron avobenzone[10] derivatives have been verified to be AIE active. Among them, the restriction of intramolecular rotation (RIR) of the phenyl rings for TPE and HPS is believed to be responsible for their AIE phenomenon[4]. On the other hand, intermolecular hydrogen-bonding interactions between polar nitrogen and/or oxygen atoms and aromatic hydrogen atoms play key roles in generating the AIE nature for cyano-stilbene and difluoroboron avobenzone species. It is well-known that molecules with different push-pull functional groups forming the donor-π-acceptor (D-π-A) backbone would have longer wavelength emission. Nowadays, it is a tendency to obtain more colorful luminogens by introducing polar groups into the skeletons of AIE molecules[11]. However, the risk of fluorescence quenching still exists in the processes of increasing the conjugated system of new AIE system. In fact, the exploration of novel AIE molecules having new parent structures and with high luminescent efficiency is still a challenging issue.

As a classical building block, 1,10-phenanthroline (phen) has been widely used in organic, inorganic and supramolecular chemistry[12-17]. The most impressive usage for phen, however, is still in coordination chemistry[18-20]. On the other hand, examples of phen based AIE compounds are seldom mentioned in the literature[21]. Numerous efforts have been made to extend the phen core in the aim of receiving functional phen derivatives. Among them, 2-(2-thienyl) imidazo[4,5-*f*]-[1,10]-phenanthroline (TIP) is a typical D-π-A molecule, which could be prepared via the condensation reaction between 1,10-phenanthroline-5,6-dione and related thiophene formaldehyde[22]. In fact, TIP species display poor solubility in common organic solvents, which will restrict their further practical applications. It is clear to us that the *N*-alkylation strategy can result in better solubility of TIP molecules and facilitate the easier purification of the resultant compounds[22-23]. By taking advantage of the dual functionality strategy, *i.e.* simultaneous imidazole *N*-alkylation of TIP and rhenium(I) tricarbonyl complexation, our group firstly reported two examples of AIEE active TIP based rhenium(I) tricarbonyl complexes[21]. It is noted that the presence of an alkyl chain in TIP compounds can impact the solid-state molecular packing conformations: (1) providing enough attachment sites for intermolecular hydrogen bonds, which is vital to fix the molecular configurations; (2) staggering the strong interlayer interactions between neighboring molecules.

In this work, 2-(5-bromo-4-methylthiophen-2-yl)-imidazo [4,5-*f*]-[1,10]-phenanthroline (1), three *N*-alkylated derivatives (**2a**~**2c**) and one related rhenium (I) tricarbonyl compound **3** were synthesized to explore the possible AIE materials (Scheme 1). Initially, the imbedment of a methyl group into the β position of thiophen unit is to improve the solubility of **1**. However, this strategy is unsuccessful. Then, a systematic investigation of *N*-alkylation for **1** has been carried out, in which three alkyl chains with different lengths (n-C_4H_9, n-C_8H_{17} and n-$C_{12}H_{25}$) were used. Indeed, the presence of *N*-alkyl tails in **2a**~**2c** can obviously enhance the solubility in common organic solvents of TIP molecules. Further X-ray single-crystal analyses of **1** and **2a**~**2c** indicated that the molecular planarity for TIP moiety could be maintained when using a short alkyl chain. The dihedral angle between

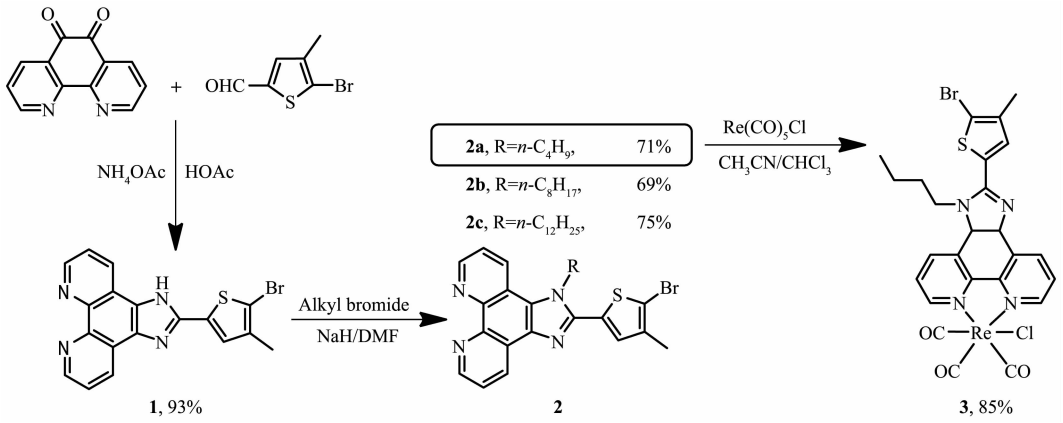

Scheme 1 Synthetic routes of *N*-alkylated TIP based compounds **2a~2c** and rhenium(I) tricarbonyl compound **3**

adjacent imidazo-[4,5-*f*]-[1,10]-phenanthroline and thiophene rings in **2a** is 10.2(5)°, which is just a bit bigger than un-alkylated **1** (2.1(8)°). At last, **2a** having the optimal balance between solubility and planarity was selected as the ligand to construct corresponding AIEE rhenium(I) tricarbonyl compound.

1 Experimental

1.1 Syntheses of the compounds

Compound **1**: 1,10-Phenanthroline-5,6-dione (3.0 g, 14.3 mmol), 5-bromo-4-methylthiophene-2-carbaldehyde (3.2 g, 15.7 mmol) and ammonium acetate (10.8 g, 140.3 mmol) were dissolved in acetic acid (50 mL) and the resulting mixture was heated at 110 ℃ for 8 h. The reaction mixture was then cooled to room temperature and neutralized by adding ammonium hydroxide until no more precipitate was formed. The precipitate was filtered through a glass fibre filter and then washed with excess water and diethyl ether. The residue was then dried in vacuo to afford compound **1** as a white solid (5.3 g, 93%). Colorless single crystals of **1** suitable for X-ray diffraction determination were grown from the mixture solution of $CH_3OH/CHCl_3$ by slow evaporation in air at room temperature for 7 days. ^{1}H NMR (500 MHz, DMSO-d_6): δ 13.91 (s, 1H), 9.03(s, 2H), 8.83~8.78 (m, 2H), 7.88~7.85 (m, 1H), 7.81~7.88 (m, 1H), 7.69 (s, 1H), 2.27 (s, 3H).

Compound **2a**: Compound **1** (1.0 g, 2.5 mmol) and NaH (0.2 g, 8.3 mmol) were dissolved in anhydrous DMF (50 mL). The resulting mixture was heated at 50 ℃ for 0.5 h, and a solution of *n*-butyl bromide (1.0 g, 7.5 mmol) in anhydrous DMF (25 mL) was added slowly. The resulting mixture was stirred overnight at 105 ℃, cooled to room temperature and quenched with water. The solution was removed under a vacuum, and then the residue was dissolved in CH_2Cl_2 (200 mL) and rinsed with distilled water for three times. The desired compound **2a** as white solid (0.8 g, 71%) was finally separated by silica gel column chromatography using $CHCl_3$ as the eluent. Colorless single crystals of **2a** suitable for X-ray diffraction determination were grown from $CHCl_3$ by slow evaporation in air at room temperature for three days. ^{1}H NMR (500 MHz, $CDCl_3$): δ 9.20~9.18 (m, 2H), 9.60 (d, 2H, *J*=8.1 Hz), 8.56 (d, 2H, *J*=8.3 Hz), 7.74~7.70 (m, 2H), 7.25 (s, 1H), 4.73 (t, 2H, *J*=8.0 Hz), 2.31 (s, 3H), 2.05~2.00 (m, 2H), 1.55~1.48 (m, 2H), 1.04 (t, 3H, *J*=7.4 Hz). ^{13}C NMR (125 MHz, $CDCl_3$): δ 149.0, 147.8, 146.4, 144.7, 144.0, 138.2, 136.7, 135.3, 130.6, 130.2, 130.0, 127.8, 125.3, 123.8, 123.5, 122.8, 122.6, 119.7, 46.8, 32.2, 19.9, 13.7, 13.6.

Compound **2b**: The synthetic procedure for **2a** was followed using **1** (1.0 g, 2.5 mmol), NaH (0.2 g, 8.3 mmol), *n*-octyl bromide (1.5 g, 7.8 mmol) and DMF (100 mL). Compound **2b** was obtained as white solid in a yield of 0.9 g (69%). Colorless single crystals of **2b** suitable for X-ray diffraction measurements were obtained from $CHCl_3$ by slow evaporation in air at room temperature for 10 days. ^{1}H NMR (500 MHz, $CDCl_3$): δ 9.19~9.16 (m, 2H), 9.04 (d, 1H, *J*=7.0 Hz), 8.52 (d, 1H, *J*=8.3 Hz), 7.74~7.68 (m, 2H), 7.23 (s, 1H), 4.70 (t, 2H, *J*=8.0 Hz), 2.30 (s, 3H), 2.06~2.00 (m, 2H),

1.49~1.43 (m, 2H), 1.36~1.27 (m, 8H), 0.89 (t, 3H, *J*= 6.7 Hz). ^{13}C NMR (125 MHz, $CDCl_3$): δ 149.1, 147.7, 146.3, 144.8, 144.2, 138.1, 136.7, 135.3, 130.4, 130.2, 130.0, 127.8, 125.2, 123.8, 123.5, 122.6, 119.7, 46.9, 31.7, 28.9, 29.1, 26.4, 22.6, 14.1, 13.7.

Compound **2c**: The synthetic procedure for **2a** was followed using **1** (1.0 g, 2.5 mmol), NaH (0.2 g, 8.3 mmol), 1-bromododecane (1.9 g, 7.6 mmol) and DMF (100 mL). Compound **2c** was obtained as a white solid in a yield of 1.1 g (75%). Colorless single crystals of **2c** suitable for X-ray diffraction measurements were obtained from $CHCl_3$ by slow evaporation in air at room temperature for 15 days. ^{1}H NMR (500 MHz, $CDCl_3$): δ 9.13~9.11 (m, 2H), 8.98 (d, 1H, *J*=8.0 Hz), 8.43 (d, 1H, *J*=8.3 Hz), 7.68~7.61 (s, 2H), 7.17 (s, 1H), 4.61 (t, 2H, *J*=7.2 Hz), 2.27 (s, 3H), 1.98 (m, 2H), 1.43 (m, 2H), 1.24 (m, 16H), 0.87 (t, 3H, *J*=6.72 Hz). ^{13}C NMR (125 MHz, $CDCl_3$): δ 149.0, 147.6, 146.2, 144.7, 144.1, 138.1, 136.5, 135.2, 130.3, 130.0, 127.6, 125.1, 123.7, 123.4, 122.5, 119.5, 46.8, 31.9, 29.6, 29.5, 29.4, 29.3, 28.9, 26.3. 22.6, 15.3, 14.1, 13.7.

Compound **3**: Compound **2a** (0.10 g, 0.22 mmol) and $Re(CO)_5Cl$ (0.11 g, 0.30 mmol) were dissolved in a mixture of CH_3CN (10 mL) and $CHCl_3$ (10 mL). The mixture was heated to reflux for 12 h and cooled to room temperature. The organic solvent was removed under a vacuum, and then the residue was dissolved in CH_2Cl_2 (50 mL) and rinsed with distilled water three times. The desired compound **3** as yellow solid (0.14 g, 85%) was finally separated by silica gel column chromatography using $CHCl_3$ as the eluent. Yellow single crystals of **3** suitable for X-ray diffraction measurements were obtained from $CHCl_3$ by slow evaporation in air at room temperature for 3 day. ^{1}H NMR (400 MHz, $CDCl_3$): δ 9.38~9.35 (m, 2H), 9.25 (dd, 1H, *J*=8.2, 1.2 Hz), 8.77 (d, 1H, *J*=8.4 Hz), 7.93~7.88 (m, 2H), 7.32 (s, 1H), 4.79 (t, 2H, *J*=8.1 Hz), 2.33 (s, 3H), 2.05~1.99 (m, 2H), 1.54~1.48 (m, 2H), 1.06 (t, 3H, *J*=7.3 Hz).

CCDC: 1992191, **1**; 1992192, **2a**; 1992193, **2b**; 1992194, **2c**; 1992195, **3**.

Table 1 Crystal data and structural refinements for five compounds

Compound	**1**	**2a**	**2b**	**2c**	**3**
Formula	$C_{19}H_{15}BrN_4OS$	$C_{23}H_{20}BrCl_3N_4S$	$C_{27}H_{28}BrCl_3N_4S$	$C_{30}H_{35}BrN_4S$	$C_{26}H_{20}BrClN_3O_3ReS$
Formula weight	427.32	570.75	626.85	563.59	756.07
T / K	291(2)	291(2)	291(2)	123(2)	291(2)
Wavelength / nm	0.071 07	0.071 07	0.071 07	0.071 07	0.071 07
Crystal size / mm	0.12×0.12×0.10	0.14×0.12×0.10	0.10×0.10×0.10	0.12×0.10×0.10	0.12×0.10×0.10
Crystal system	Orthorhombic	Triclinic	Monoclinic	Triclinic	Orthorhombic
Space group	$P2_12_12_1$	$P\bar{1}$	*C*2/*c*	$P\bar{1}$	*Pbca*
a / nm	0.570 7(1)	0.934 7(2)	3.334 2(8)	0.739 6(2)	1.482 1(1)
b / nm	1.344 1(2)	1.098 8(2)	0.728 7(2)	0.923 0(2)	1.058 7(1)
c / nm	2.262 7(4)	1.266 1(3)	2.712 3(9)	2.127 1(5)	3.141 5(1)
α / (°)		107.669(3)		89.481(4)	
β / (°)		103.561(3)	119.057(19)	88.705(3)	
γ / (°)		94.534(4)		70.839(4)	
V / nm^3	1.735 8(5)	1.188 5(4)	5.760(3)	1.371 3(5)	4.929 0(2)
Z	4	2	8	2	8
D_c / (g·cm^{-3})	1.635	1.595	1.446	1.365	2.038
F(000)	864	576	2 560	588	2 912
μ / mm^{-1}	2.505	2.174	1.802	1.601	6.781
h_{min}, h_{max}	−6, 6	−11, 11	−39, 36	−20, 20	−18, 19
k_{min}, k_{max}	−13, 15	−13, 12	−6, 8	−11, 11	−13, 13
l_{min}, l_{max}	−25, 26	−13, 15	−32, 32	−25, 23	−34, 40

Continued Table 1

Data, parameter	3 050, 238	4 151, 319	5 060, 326	4 789, 326	5 660, 327
Final *R* indices [$I>2\sigma(I)$]*	R_1=0.105 9, wR_2=0.291 2	R_1=0.078 9, wR_2=0.208 3	R_1=0.109 7, wR_2=0.247 8	R_1=0.104 4, wR_2=0.239 4	R_1=0.038 6, wR_2=0.091 0
R indices (all data)	R_1=0.125 0, wR_2=0.310 0	R_1=0.098 6, wR_2=0.218 3	R_1=0.249 1, wR_2=0.282 1	R_1=0.158 7, wR_2=0.262 3	R_1=0.056 9, wR_2=0.100 2
S	1.286	1.068	1.194	0.950	1.068
$(\Delta\rho)_{max}$, $(\Delta\rho)_{min}$ / (e·nm^{-3})	1 829, −1 052	995, −1 378	591, −861	629, −1 262	1 252, −2 364

*$R_1=\sum||F_o|-|F_c||\sum|F_o|$, $wR_2=\{\sum[w(F_o^2-F_c^2)^2]\sum w(F_o^2)^2\}^{1/2}$

2　Results and discussion

2.1　Syntheses

As shown in Scheme 1, precursor **1** was prepared via the Debus-Radziszewski reaction in a high yield of 93%. Similar to the known 2-(5-bromothiophen-2-yl)-imidazo[4,5-*f*]-[1,10]-phenanthroline[22], compound **1** shows poor solubility in common organic solvents, which may be due to the existence of proton in the imidazole unit. Compounds **2a**~**2c** having the same skeleton but different alkyl tails (*n*-C_4H_9, *n*-C_8H_{17} and *n*-$C_{12}H_{25}$) were obtained via the *N*-alkylation reactions between **1** and corresponding alkyl bromides in satisfactory yields. All new organic compounds herein have been verified by NMR spectra and X-ray single-crystal structural analyses. It is found that the solubility of *N*-alkylated compounds is significantly increased with the increase of alkyl chain lengths. Herein, compound **2a** was used as the bidentate chelating ligand for preparing tricarbonyl Re(I) compound **3**. The reaction between $Re(CO)_5Cl$ and **2a** in $CH_3CN/CHCl_3$ under the refluxing condition afforded compound **3**. Because of the presence of an alkyl chain, compound **3** shows good solubility in common organic solvents and could be further purified by column chromatography. As can be seen in Fig.1,

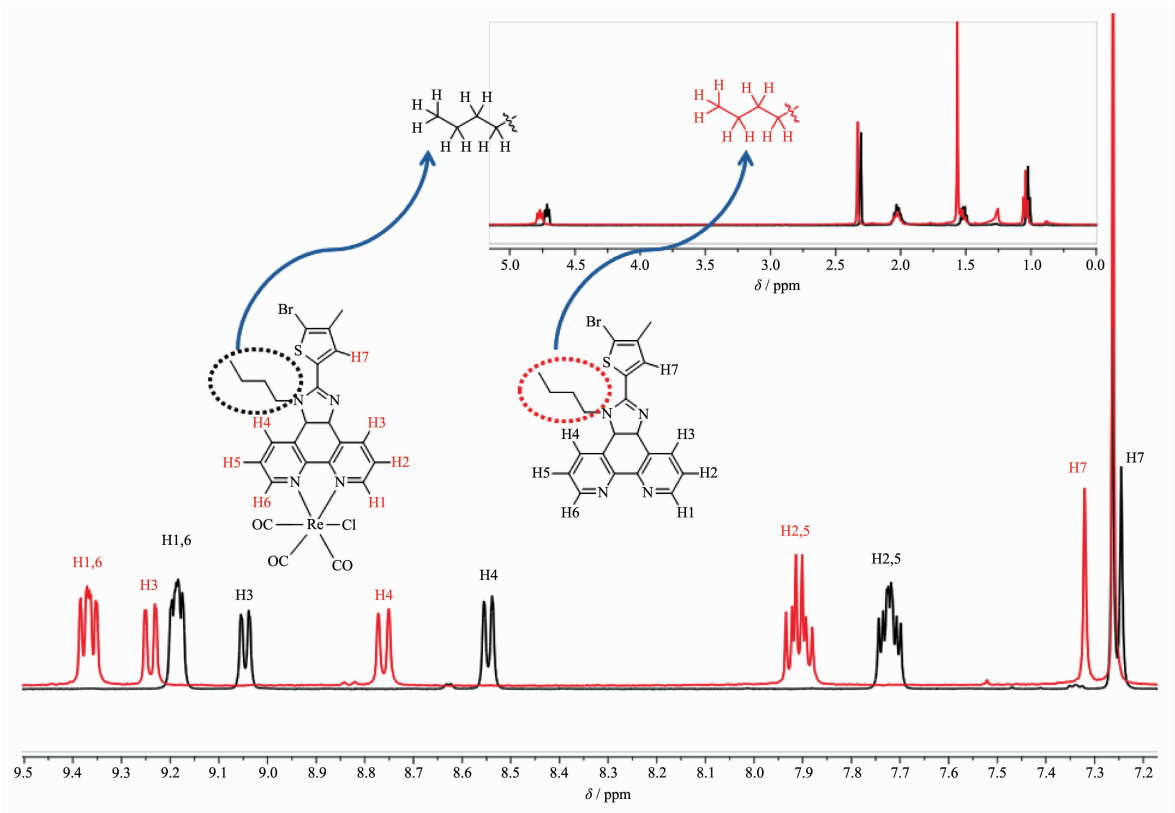

Fig.1　Comparative ^{1}H NMR spectra for compound **2a** and its Re(I) compound **3**

all characteristic proton signals of **3** are shifted to lower fields in comparison with its free ligand **2a** because of the deshielding effects from the rhenium(I) center. Especially, the $\Delta\delta$ values for phen protons are larger than others because the lone pair electrons of two nitrogen atoms of phen are more closer to Re(I) center, thus exhibiting stronger deshielding effects.

2.2 Spectral characterizations

For the sake of comparison, electronic absorption behaviors of **2a**~**2c** in solution were recorded at the same concentration of 50 μmol·L^{-1} (Fig.2). Generally, TIP could be considered as a typical D-π-A molecule, where the electron deficient phenanthroline part is fused with an imidazole ring and bridged by an electron-rich thiophene ring. The maximum absorption peak around 327 nm can be assigned as the π-π* transition absorption of the conjugated system. It is noted that compounds **2a**~**2c** with different alkyl chains show very similar UV-Vis absorptions since all of them have similar molecular conjugation system.

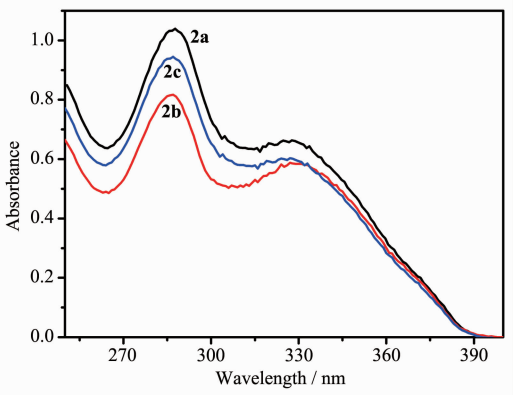

Fig.2 UV-Vis absorption spectra of compounds **2a**~**2c** in dichloromethane at room temperature with the same concentration of 50 μmol·L^{-1}

Similar to most of phen based rhenium (I) tricarbonyl complexes, herein, **3** only displayed very dark red emission in organic solvent[21,24]. On the other hand, the solid sample of **3** showed stronger photoluminescence (PL) intensity than that in solution. The distinguishing PL property between solid and solution states hints the possible AIEE nature of **3**. So the aggregation behavior of **3** was further studied via recording the PL spectra in acetone/water under various volume fractions of water, f_w (Fig.3). The pure acetone solution of **3** exhibited weak emission at 606 nm when excited at 365 nm. When the f_w value was increased from 0 to 40% gradually, no obvious changes in the PL spectra could be observed. By further increasing the water fraction (40% and 50%), the PL intensity was slightly increased, indicative of the formation of aggregates. The highest fluorescence intensity for Re(I) compound **3** could be recorded at f_w=80%, therefore testifying the AIEE property. However, a slight decline in the PL intensity was found when f_w value reached to 90%, and significant precipitants could be observed in the solution.

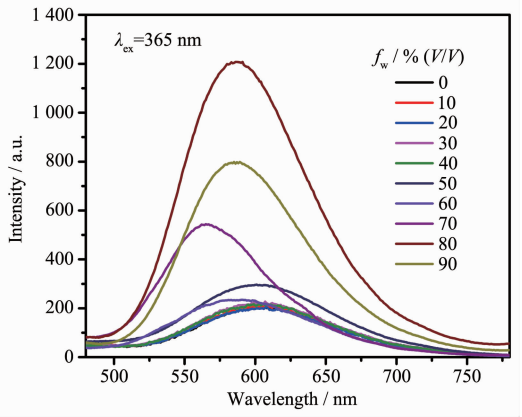

Fig.3 Fluorescence emission for Re(I) compound **3** in acetone/water mixtures with the same starting concentration of 30 μmol·L^{-1} and different water volume fractions (f_w)

2.3 Single-crystal structures and AIE mechanism

Compared with the traditional characterization methods, X-ray single-crystal diffraction technique could afford a deeper insight into compounds especially for the molecular geometry and packing[25]. Herein, we have obtained the single-crystal structures of organic compounds **1**, **2a**~**2c** and compound **3**. The molecular structures with the atom-numbering scheme of **1**, **2a**~**2c** are shown in Fig.4. Compound **1** has an additional methyl group in the thiophene ring in comparison with the classical 2-(5-bromothiophen-2-yl)-imidazo[4,5-*f*]-[1,10]-phenanthroline. In **2a**~**2c**, the implanted *N*-alkyl chains and the neighboring sulfur atom of the thiophene ring are found to point the opposite directions, thus displaying the *trans* configuration. It is known that the planarity of the

entire molecule has a close relation to the photophysical property of the D-π-A compound. Herein, the whole molecule of **1** adopts the planar conformation, in which the dihedral angle between the imidazo[4,5-*f*]-[1,10]-phenanthroline moiety and its neighboring thiophene ring is as small as 2.1(8)°. However, the above-mentioned dihedral angles are slightly increased to 10.2(5)° in **2a** and 13.4(7)° in **2b**, respectively, while it is significantly increased to 38.0(9)° in **2c**. In other words, the introduction of different *N*-alkyl chains into the imidazole ring in TIP molecules could increase the afore-mentioned dihedral angles to different extents owing to the steric hindrance effects of alkyl chains.

As can be seen in Fig.5a, the six-coordinated rhenium(I) center in **3** adopts the distorted octahedral geometry, which is constituted by one chlorine counterion, two nitrogen atoms from phen and three carbonyl ligands in the fac arrangement. Similar to its ligand, the thiophene sulfur atom and the implanted *N*-alkyl chain in **3** pointing toward the opposite

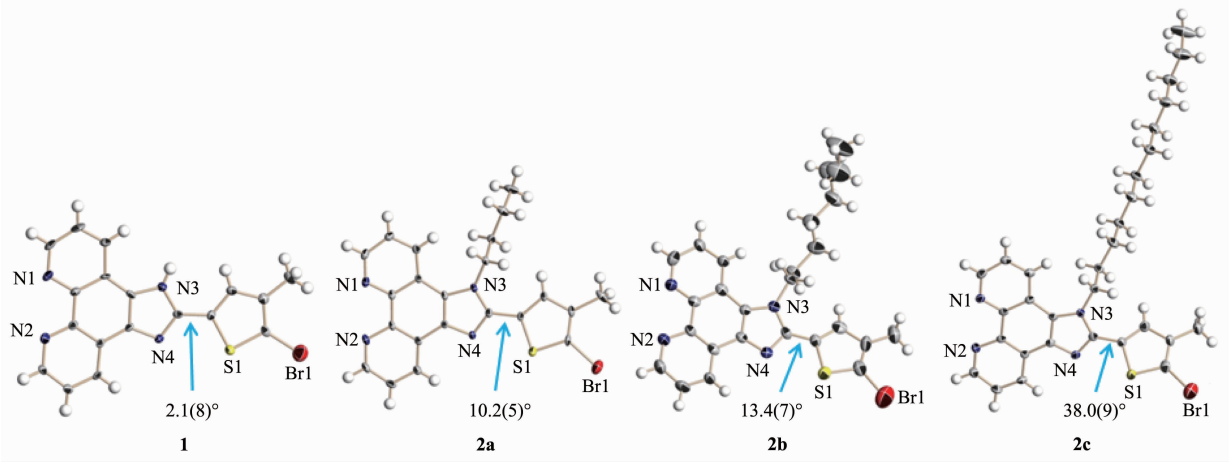

All the solvent molecules are omitted for clarity

Fig.4　ORTEP diagrams (30% thermal probability ellipsoids) for the molecular structures of **1**, **2a**, **2b** and **2c**, showing the relative configuration and related dihedral angles between adjacent aromatic heterocycles

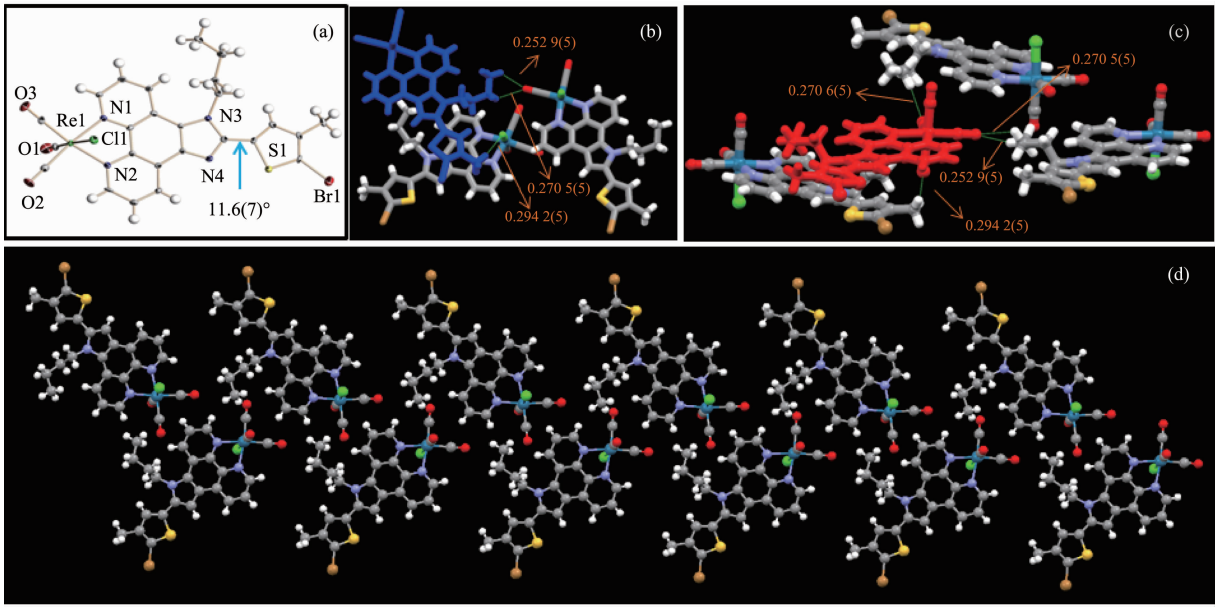

Fig.5　(a) ORTEP diagram (30% thermal probability ellipsoids) for compound **3** showing the relative configuration and related dihedral angles between adjacent aromatic heterocycles; (b, c) Hydrogen-bonding interactions (nm) in the single-crystal lattice of **3**; (d) Packing structure of **3**

directions adopting the trans configuration as well. The dihedral angle between imidazo [4,5-*f*]-[1,10]-phenanthroline and its neighboring thiophene ring in **3** is 11.6(7)°, which is slightly larger than its free ligand **2a** (10.2(5)°). As shown in Fig.5b and 5c, every molecule in **3** connects with three adjacent ones via multiple intermolecular C –H ⋯ O and C –H ⋯ Cl hydrogen-bonding interactions. The chlorine and one carbonyl oxygen atoms of the distorted octahedral structure work as the stators to connect their adjacent hydrogen atoms from the *N*-alkyl chain and thiophen methyl group. Moreover, molecules of **3** are assembled into loose two dimensional networks via synergistic effects of crowding *N*-alkyl chains and distoreted octahedral geometry, in which no typical π-π stacking could be found (Fig.5d).

As discussed in the above-mentioned structural analysis, it is concluded that the AIEE effect of compound **3** is associated with its molecular conformation and packing mode in the solid state: (1) the fixation effect from multiple intermolecular C–H⋯O and C–H⋯Cl hydrogen-bonding interactions in **3** is suggested to restrict the non-radiative channel and activate the radiative pathway; (2) the twisted conformation from the rhenium(I) octahedral geometry as well as the presence of crowding *N*-alkyl chain of **3** will help to prevent the formation of close stacking in their condensed state, which is also beneficial for the solid-state PL emission. When aggregated into nanosuspensions, the intramolecular free rotations for aryl rotors of the whole molecules in **3** are restricted, thus resulting in the observed AIEE phenomenon.

3 Conclusions

In this work, systematic investigations on the *N*-alkylation of 2-(5-bromo-4-methylthiophen-2-yl)-imidazo [4,5-*f*]-[1,10]-phenanthroline (**1**) have been performed. As a result, three *N*-alkylated TIP based derivatives **2a**~**2c** with different alkyl chains (*n*-C_4H_9, *n*-C_8H_{17} and *n*-$C_{12}H_{25}$) have been obtained. It is found that the introduction of an *N*-alkyl group into the imidazole ring can obviously improve the solubility of this family of TIP compounds. X-ray single-crystal analyses reveal that the presence of different *N*-alkyl chains in **2a**~**2c** can increase the dihedral angles between imidazo [4,5-*f*]-[1,10]-phenanthroline and its neighboring thiophene ring in different extents. Among them, compound **2a** with the shortest alkyl tail was used as the ligand to construct the rhenium(I) tricarbonyl compound **3**. The AIEE effect of **3** was further verified by recording the PL spectra in the acetone/water mixtures with different fractions of water. Further X-ray single-crystal analysis of **3** indicate that the existence of loose packing mode and the multiple intermolecular hydrogen-bonding interactions can guarantee the generation of AIEE activity of **3**. This work is suggested to throw some new lights on the exploring of AIEE materials via the combination of imidazole *N*-alkylation and rhenium (I) tricarbonyl complexation.

Supporting information is available at http://www.wjhxxb.cn

References:

[1] Luo J, Xie Z, Lam J W Y, et al. *Chem. Commun.*, **2001**:1740-1741

[2] Hong Y, Lama J W Y, Tang B Z. *Chem. Commun.*, **2009**,**1**:4332-4353

[3] Mei J, Leung N L C, Kwok R T K, et al. *Chem. Rev.*, **2015**, **115**:11718-11940

[4] Kwok R T K, Leung C W T, Lam J W Y, et al. *Chem. Soc. Rev.*, **2015**,**44**:4228-4238

[5] Yoon S J, Chung J W, Gierschner J, et al. *J. Am. Chem. Soc.*, **2010**,**132**:13675-13683

[6] Chi Z, Zhang X, Xu B, et al. *Chem. Soc. Rev.*, **2012**,**41**:3878-3896

[7] Zhao N, Zhang C, Lam J W Y, et al. *Asian J. Org. Chem.*, **2014**,**3**:118-121

[8] Feng W Q, Su Q, Ma Y, et al. *J. Org. Chem.*, **2020**,**85**:158-167

[9] Xue P, Zhang C, Wang K, et al. *Dyes Pigm.*, **2019**,**163**:516-524

[10]Galer P, Korosec R C, Vidmar M, et al. *J. Am. Chem. Soc.*, **2014**,**136**:7383-7394

[11]Wang J, Mei J, Hu R, et al. *J. Am. Chem. Soc.*, **2012**,**134**:9956-9966

[12]Hiort C, Lincoln P, Norden B. *J. Am. Chem. Soc.*, **1993**, **115**:3448-3454

[13]Brodie C R, Collins J G, Aldrich-Wright J R, et al. *Dalton Trans*., **2004**:1145-1152

[14]Carney J M, Donoghue P J, Wuest W M, et al. *Org. Lett*., **2008**,**10**:3903-3906

[15]Accorsi G, Listorti A, Yoosaf K, et al. *Chem. Soc. Rev*., **2009**,**38**:1690-1700

[16]Chelucci G, Thummel R P. *Chem. Rev*., **2002**,**102**:3129-3170

[17]Ge Z, Hayakawa T, Ando S, et al. *Org. Lett*., **2008**,**10**:421-424

[18]Chen X Y, Yang X P, Holliday B J. *J. Am. Chem. Soc*., **2008**,**130**:1546-1547

[19]Li Y H, Dandu M, Liu R, et al. *J. Phys. Chem. C*, **2014**, **118**:6372-6384

[20]Liu Y, Wang Y F, Guo H P, et al. *J. Phys. Chem. C*, **2011**, **115**:4209-4216

[21]Liu H Q, Peng Y X, Zhang Y, et al. *Dyes Pigm*., **2020**,**174**:108074

[22]Peng Y X, Wang N, Dai Y, et al. *RSC Adv*., **2015**,**5**:6395-6406

[23]Peng Y X, Tao T, Wang X X, et al. *Chem. Asian J*., **2014**,**9**:3593-3603

[24]Peng Y X, Xu D, Wang N, et al. *Tetrahedron*, **2016**,**72**:3443-3453

[25]Peng Y X, Liu H Q, Shi R G, et al. *J. Phys. Chem. C*, **2019**, **123**:6197-6204